This article has been accepted for inclusion in a future issue of this journal. Content is final as presented, with the exception of pagination.

Development of a *Ka*-Band Circular TM_{01} to Rectangular TE_{10} Mode Converter

Qingyun Chen, Xuesong Yuan, Tongbin Yang, Jie Xie, Xiaotao Xu, Bin Wang, Hailong Li, Yong Yin, Matthew T. Cole, Lin Meng, and Yang Yan

***Abstract*—The output/input circuit is a core component in all high-power millimeter-wave (MMW) radiation sources, and its performance specifications and reliability directly impact upon the performance of the radiation source device. Central to achieving high power is the development of efficient mode converters. Here, we report on the development of a compact *Ka*-band circular TM_{01} to rectangular TE_{10} mode converter. The present mode converter adopts an all-metal waveguide structure and facilitates notable improvement in the system power capacity and is capable of realizing high-power propagation. The mode converter realizes effective mode conversion between high-order and fundamental modes, as well as allowing longitudinal and transverse transmission. Our simulation and empirical findings have shown mode purity ≥99.5% in the frequency range of 32.7–34.6 GHz, and the mode conversion efficiency is more than 96% at a center frequency of 32.9 GHz with a return loss S_{11} of −19.3 dB. The bandwidth of the converter is 2.4 GHz with transmission coefficient $S_{21} \geq -1$ dB.**

***Index Terms*—Circular TM_{01} mode, high-power radiation source, mode converter *Ka*-band, rectangular TE_{10} mode.**

I. Introduction

HIGH-POWER microwave and millimeter-wave (MMW) vacuum electronic devices (VEDs) have a considerably wide range of applications; from radar systems and high data rate communications, and nondestructive industrial detection methods, to remote high-resolution imaging in materials research, deep space research, and communications devices. To date, some high-power MMW VEDs operate using circular waveguides and high-order circular TM_{01} mode in order to achieve the required high power capacity [1]–[3]. In order to achieve improved radiation directionality, multi-channel coupling, and enhanced space transmission, mode converters are commonly employed to convert high-order modes to the rectangular waveguide fundamental mode-TE_{10} which has a peak gain at the aperture in their radiation patterns, hence, high propagation stability [4]–[6]. Several high-power radiation systems pump in or pump out radio frequency (RF) energy in the rectangular TE_{10} mode to achieve this [7]–[9], and the mode excitation of some antennas requires the rectangular TE_{10} mode. The rectangular TE_{10} mode itself has a relatively wide range of applications [10], [11]. There is a clear practical need, which has yet to be met, for the development of an electromagnetic wave conversion circuit that converts circular waveguide high-order mode-TM_{01} to rectangular waveguide fundamental mode-TE_{10}. Nevertheless, many challenges presently hinder the development of mode converters in high-power radiation devices. Amongst these, perhaps the most pressing is ensuring that the transmission of the RF energy to the load or external circuitry in the desired mode is achieved with a high conversion efficiency and mode purity. The mode converter must offer wide bandwidth and high mode purity in order to withstand frequency instabilities. Given the use of such a system in mass-critical application, compactness, dependability, and easy integration of the mode conversion system are also critical design considerations.

Incumbent conventional mode converters to date employ serpentine, sectoral, or dual bent circular waveguide structures which are difficult to fabricate and install [12]–[14]. New mode converter structure loaded with dielectric, metallic photonic crystals, and coaxial waveguide structures have also been recently reported [15]–[17]. Due to a variety of functional limitations of these structures, including voltage breakdown of medium, small cavity, and dielectric loss, many such mode converters are incapable of sustaining high-power microwave or MMW emission compared with more traditional all-metal mode converters that are better suited for use in potentially high-power radiation sources including Plasma Assisted Slow Wave Oscillators (Pasotron) [18]–[20], Cerenkov [21], and Traveling Wave Amplifier [22].

In this article, we have a report on the development of a *Ka*-band mode converter for conversion between the circular TM_{01} and rectangular TE_{10} modes. The proposed mode converter is based on an all-metal waveguide structure that improves the power capacity of device markedly over other material platforms. The specific sidewall coupled input–output structure has been employed to realize a

Manuscript received November 21, 2019; revised December 20, 2019, January 14, 2020, and January 16, 2020; accepted January 17, 2020. This work was supported in part by the National Key Research and Development Program of China under Grant 2019YFA0210202, in part by the National Natural Science Foundation of China under Grant 61771096, and in part by the Fundamental Research Funds for the Central Universities under Grant ZYGX2019Z006 and Grant ZYGX2019J012. The review of this article was arranged by Editor M. Thumm. *(Corresponding author: Xuesong Yuan.)*

Qingyun Chen, Xuesong Yuan, Tongbin Yang, Jie Xie, Xiaotao Xu, Bin Wang, Hailong Li, Yong Yin, Lin Meng, and Yang Yan are with the School of Electronic Science and Engineering, University of Electronic Science and Technology of China, Chengdu 610054, China (e-mail: cqy@std.uestc.edu.cn; yuanxs@uestc.edu.cn).

Matthew T. Cole is with the Department of Electronic and Electrical Engineering, University of Bath, Bath BA2 7AY, U.K. (e-mail: m.t.cole@bath.ac.uk).

Color versions of one or more of the figures in this article are available online at http://ieeexplore.ieee.org.

Digital Object Identifier 10.1109/TED.2020.2968347

This article has been accepted for inclusion in a future issue of this journal. Content is final as presented, with the exception of pagination.

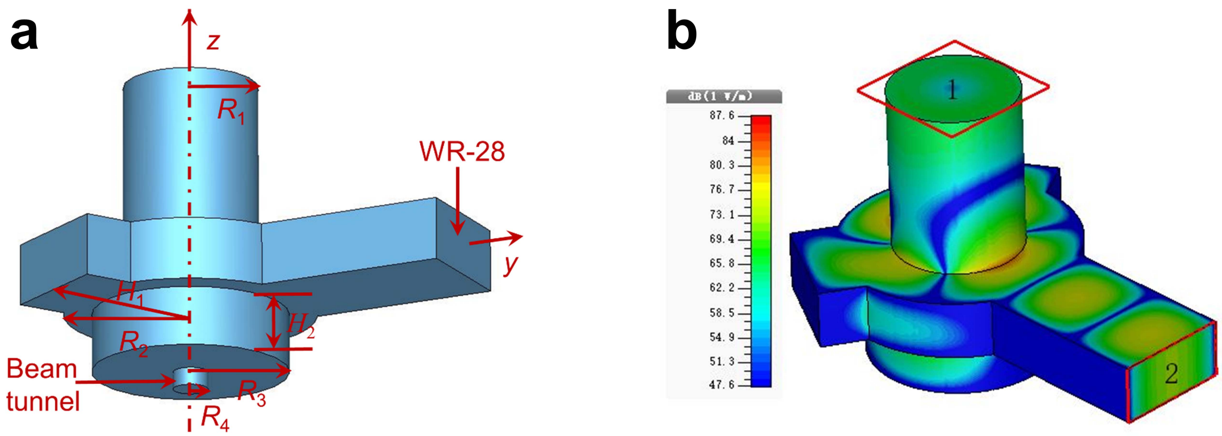

Fig. 1. (a) 3-D rendering of the vacuum enclosure of the mode converter. (b) Electric field distributions in the mode converter when the TM_{01} is fed in port 1 and TE_{10} is output from port 2.

TABLE I
MODE CONVERTER DIMENSIONS

Symbol	Quantity	Dimension(mm)
R_1	radius of the input circular waveguide	3.92
R_2	radius of coupled circular waveguide	7.27
R_3	radius of circular waveguide short-circuit plane	5.65
R_4	radius of beam tunnel	1
H_1	distance between the rectangular waveguide short-circuit plane and the z axis	9.23
H_2	length of circular waveguide short-circuit plane	3.4

transverse input–output high transmission efficiency of 96%. Our experimental and simulation results demonstrate that the developed mode converter has many significant advantages such as simple circuit structure, facile manufacturability, low cost, convenient installation, low-attenuation, high mode purity, wide operating bandwidth, and considerable conversion efficiency, highlighting the converters wider usefulness in high-power VEDs.

II. SIMULATION

The 3-D rendering of the sidewall coupled output mode converter vacuum enclosure is shown in Fig. 1(a). The mode converter has two ports; a circular waveguide (port 1) and a rectangular waveguide (port 2). In order to obtain high mode conversion efficiency, the design geometries of the mode converter are determined after a series of optimized parametric simulations. From this article, we find the following optimized geometries; the radius of the input circular waveguide R_1, the radius of coupled circular waveguide R_2, the radius of circular waveguide short-circuit plane R_3, and the radius of beam tunnel R_4, the distance between the rectangular waveguide short-circuit plane and the z-axis H_1, and the length of circular waveguide short-circuit plane is H_2 are listed in Table I. The output rectangular waveguide and rectangular waveguide short-circuit plane are standard WR-28 waveguides (7.11 mm × 3.56 mm).

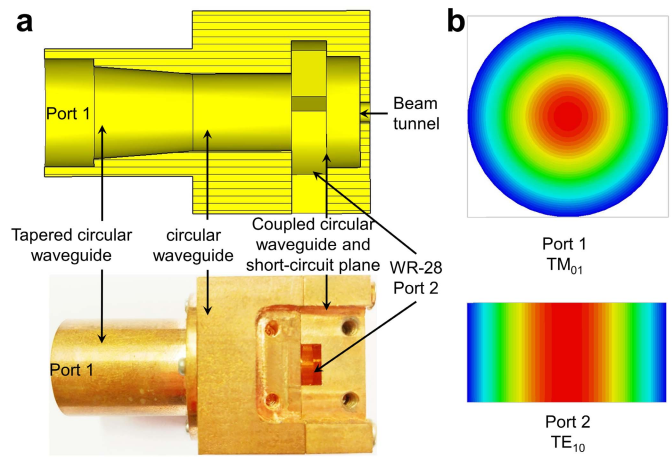

Fig. 2. (a) Cross section schematic and photograph of the circular TM_{01}-rectangular TE_{10} mode converter. (b) Field distributions of circular TM_{01} mode and rectangular TE_{10} mode on port 1 and port 2.

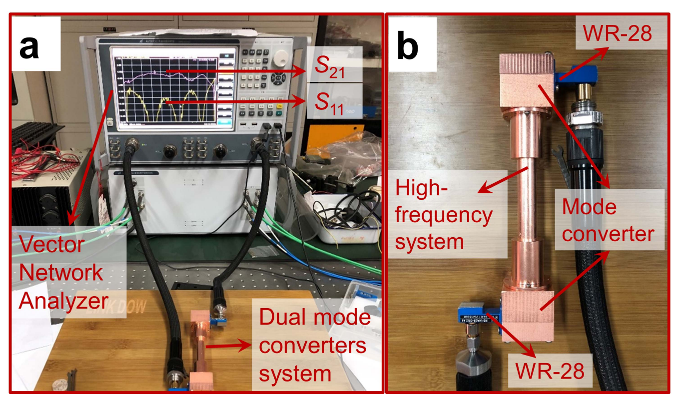

Fig. 3. (a) Photograph of the experimental setup and typical S_{11} and S_{21} experimental results. (b) Dual mode converter measurement setup, symmetrically connected through a high-frequency system.

The transmission characteristics of the mode converter are simulated using a commercial time-domain simulation package (CST Microwave Studio). Fig. 1(b) depicts the electric field distribution in the mode converter when the circular TM_{01} mode is fed into port 1 and the rectangular TE_{10} mode is output from port 2. Our simulations demonstrate that the

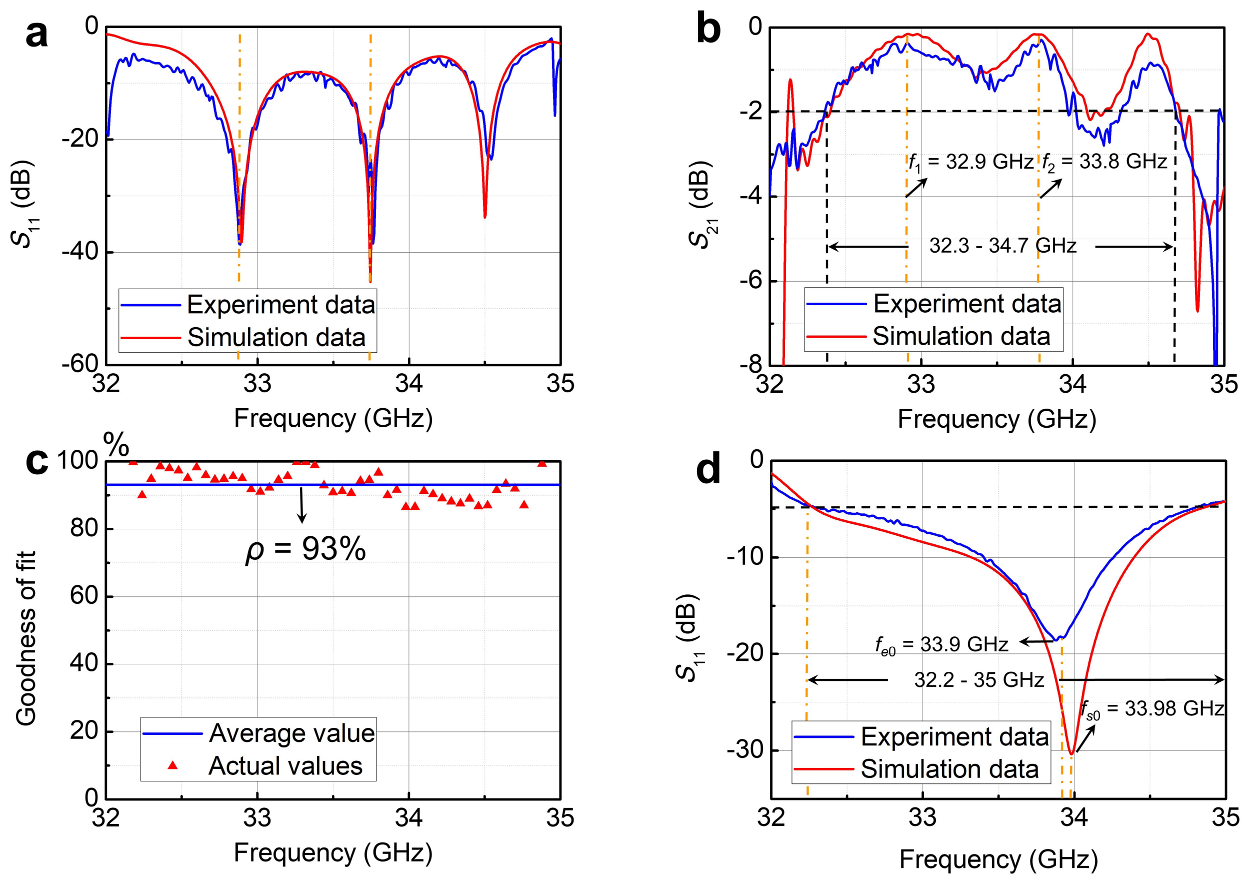

Fig. 4. Comparison of experimental and simulation results of (a) S_{11} and (b) S_{21} of the dual mode converters. (c) Goodness of fit of S_{21} between experimental and simulation results. (d) S_{11} of the single mode converter.

propagation direction of the electromagnetic wave has been transformed, with a peak magnitude field at the aperture at port 2. Here, we use the S_{11} and S_{21} scattering coefficients to describe the transmission characteristics for the different operating frequencies. The simulated results and analyses of conversion efficiency, mode purity, and power capacity of the mode converter are presented in Section IV.

III. Experiment

The proposed mode converter comprises a top circular waveguide (port 1), a circular waveguide short-circuit plane with a beam tunnel, a middle coupled circular waveguide, and three rectangular waveguides placed at 120° at the intersection of the coupled section. Two of these waveguides are rectangular waveguide short-circuit planes and one is the output rectangular waveguide (port 2). A cross-sectional schematic and photograph of the manufactured mode converter are shown in Fig. 2(a). The mode converter is processed in three parts: a tapered circular waveguide, an input circular waveguide, and a coupled circular waveguide connected to a short-circuit plane. A tapered circular waveguide is attached to the input circular waveguide of the mode converter to match the output port of an existing high-frequency structure in our present laboratory setup. Fig. 2(b) shows the circular TM_{01} mode and rectangular TE_{10} mode field distributions at port 1 and port 2 within the converter. The transmission characteristics of the mode converter are measured using a vector network analyzer (VNA, Make: China Electronics Technology Instruments Co., Ltd., Model: AV3672C), as shown in Fig. 3(a). Since the measurement ports of the VNA are international standardized WR-28 ports, two mode converters are symmetrically connected through a high-frequency system in the experimental measurement, as shown in Fig. 3(b). The display screen of the VNA in Fig. 3(a) shows typical S-parameters measurement in dB. Since a dual mode converter test is adopted, the S-parameter values of a single mode converter is necessarily half of the measured experimental data. Our experimental results demonstrate that our circular TM_{01} to rectangular TE_{10} mode converter has transmission coefficient S_{21} of ≥ -1 dB in the range of 32.3–34.7 GHz as shown in Fig. 4(b). The S_{11} of a single mode converter is also tested, as shown in Fig. 4(d). These findings demonstrate that $S_{11} < -5$ dB in the range of 32.2–35.0 GHz, and as low as −19 dB at 33.9 GHz. The analyses of experimental data of the mode converter are presented in Section IV.

IV. Results and Discussion

The simulated conversion efficiency of the mode converter is plotted in Fig. 5(a). S_{11}, S_{21}, and mode purity have been simulated across the frequency range of 32–36 GHz. At a center frequency of 32.73 GHz, the transmission coefficient S_{21} is ~0, and the reflection coefficient $S_{11} = -17$ dB. The bandwidth of $S_{21} \geq -1$ dB is from 32.4 to 35.0 GHz. Fig. 5(b) shows the variation of mode purity as a function of frequency.

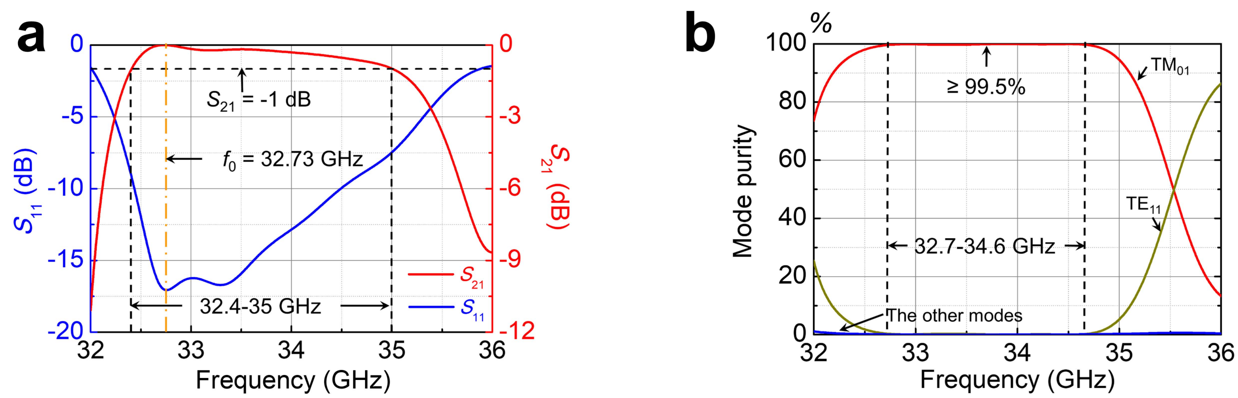

Fig. 5. Mode converter simulation results. (a) S-parameters of the mode converter. (b) Variation of mode purity as a function of frequency.

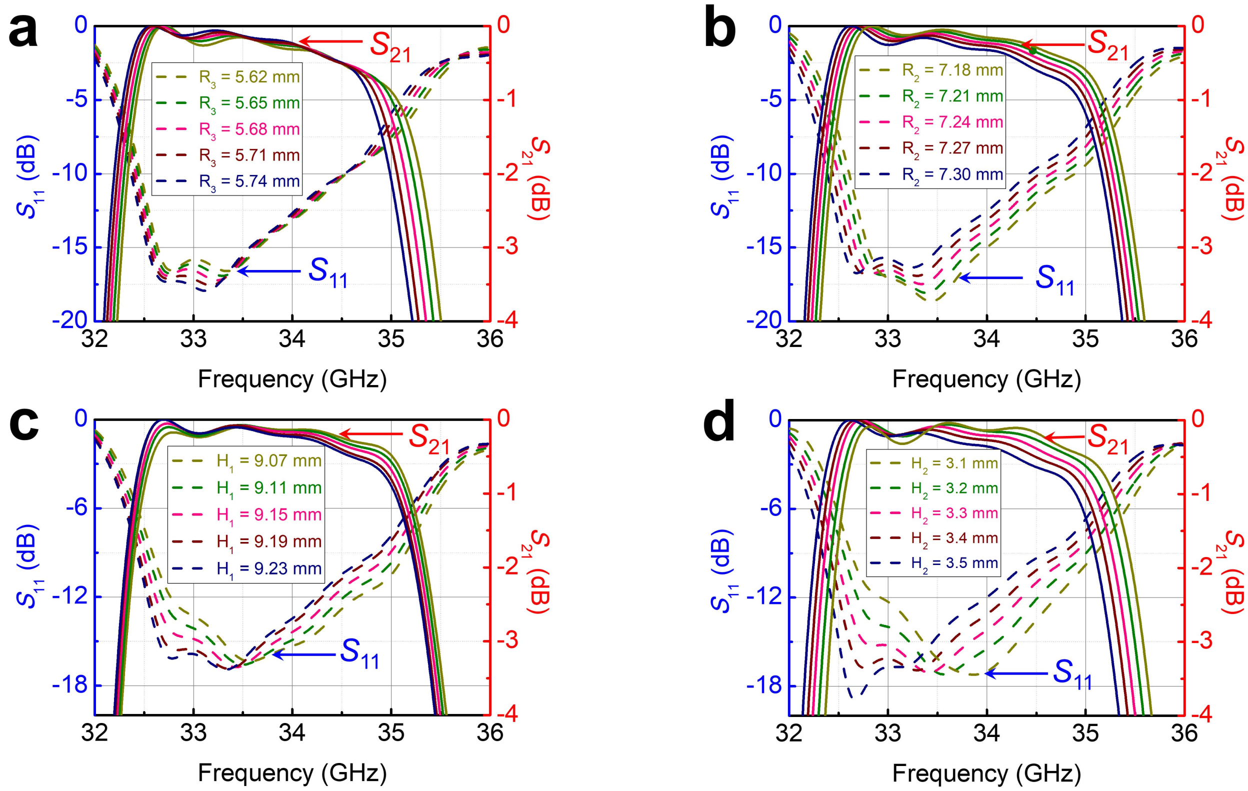

Fig. 6. Parametrically optimized S-parameters of the mode converter as a function of enclosure geometry. (a) Radius of circular waveguide short-circuit plane R_3. (b) Radius of coupled circular waveguide R_2. (c) Distance between the rectangular waveguide short-circuit plane and the z-axis H_1. (d) Length of circular waveguide short-circuit plane is H_2.

The mode purity of the TM_{01} mode is as seen to be as high as $\geq$99.5% in the frequency range of 32.7–34.6 GHz. When the frequency exceeds 35.0 GHz, the TE_{11} mode rapidly increases and dominates. The mode converter has a notable mode purity in our operating frequency range. Moreover, we have estimated the power capacity of the mode converter by using simulation software. The incident power of 1 W in the mode converter possesses the max E-field $E_m = 4.2$ kV/m at a center frequency of 32.7 GHz. Therefore, power capacity is estimated as 500 kW (air breakdown threshold $E_t = 3$ MV/m) [23].

Simulation optimizations have been conducted to explore the influence of the structural parameters on the transmission characteristics, as shown in Fig. 6. Several dominant parameters have been considered, specifically the radius of the coupled circular waveguide R_2, the radius of the circular waveguide short-circuit plane R_3, the distance between the rectangular waveguide short-circuit plane and the z-axis H_1, and the length of the circular waveguide short-circuit plane H_2. The simulation results illustrate that the bandwidth increases linearly as R_3, R_2, H_1, and H_2 decrease. However, reducing R_3 and H_2 results in S_{21} fluctuating dramatically, whilst reducing R_3 reduces the transmission efficiency. Though causing slight fluctuations in S_{21}, reducing R_2 and H_1 can be selected to smooth the transmission coefficient though this reduces the transmission efficiency at center frequency. Our studies suggest an optimal R_3 of 5.65 mm, R_2 of 7.27 mm, H_1 of 9.23 mm, and H_2 of 3.4 mm which are used herein to ensure that the transmission coefficient S_{21} remains suitably smooth while retaining a high transmission efficiency (96%) and a broad bandwidth (2.4 GHz).

Our experimental and simulation S-parameter data are plotted in Fig. 4(a), (b), and (d). The simulation and analytical results for the power transmitted through the mode converter and power reflected at the input port are seen to be in ~93% agreement with our experimentally measured results as shown in Fig. 4(c). Moreover, we find two frequencies with peak conversion efficiency (32.9 and 33.8 GHz), as shown in Fig. 4(a) and (b). At the 32.9 GHz peak, $S_{21} = -0.18$ dB, and $S_{11} = -19.3$ dB with a goodness of fit of 95%. The measured conversion efficiency between circular TM_{01} mode and rectangular TE_{10} mode is up to 96%. At the 33.8-GHz peak, $S_{21} = -0.15$ dB, $S_{11} = -14.2$ dB with a high goodness of fit of 96.7%, and the conversion efficiency between the two modes is up to 97%. Fig. 4(b) shows that the curve of S_{21} has several valleys and peaks resulting from resonant frequencies within the high-frequency cavity. In the previous simulations, we demonstrate that S_{21} of a single mode converter has a smooth frequency profile with a bandwidth of -1 dB. Fig. 4(d) shows a 0.23% error of center frequency between experimental and simulation results. There is a cavity in port 1 as shown in Fig. 2(a), used to connect high-frequency structure. In experimental measurement of a single mode converter, resonant characteristic of the cavity results in the small error of center frequency.

V. Conclusion

In this article, a *Ka*-band mode converter has been designed and successfully manufactured that is capable of realizing the conversion between circular TM_{01} and rectangular TE_{10} modes. Experimental and simulation results collectively show that the frequency bandwidth is 2.4 GHz with a transmission coefficient $S_{21} \geq -1$ dB, across a frequency range of 32.3–34.7 GHz. The proposed mode converter has good performance at a center frequency of 32.9 GHz with a high conversion efficiency—transmission coefficient S_{21} which can reach up to -0.18 dB, with a return loss S_{11} as low as -19.3 dB, and a modal conversion efficiency of up to 96%. The mode purity of circular TM_{01} mode has been shown to be $\geq$99.5% in the operating frequency range. In addition, the mode converter with no beam tunnel can be connected to the external circuit to act as external output device. The development of mode converters with such high conversion efficiency and high mode purity open up an exciting landscape for future development of a new generation of traveling tubes (TWTs), klystrons, extended interaction klystrons (EIKs), and backward wave oscillators (BWOs) that have the potential to produce output powers in excess of hundreds of kilowatt level in *Ka*-band.

References

[1] Q. Chen, X. Yuan, M. Cole, Y. Zhang, L. Meng, and Y. Yan, “Theoretical study of a 0.22 THz backward wave oscillator based on a dual-gridded, carbon-nanotube cold cathode,” *Appl. Sci.*, vol. 8, no. 12, p. 2462, Dec. 2018, doi: 10.3390/app8122462.

[2] C. Chen, G. Liu, W. Huang, Z. Song, J. Fan, and H. Wang, “A repetitive X-band relativistic backward-wave oscillator,” *IEEE Trans. Plasma Sci.*, vol. 30, no. 3, pp. 1108–1111, Jun. 2002, doi: 10.1109/TPS.2002.801656.

[3] M. Friedman, J. Krall, Y. Y. Lau, and V. Serlin, “Efficient generation of multigigawatt rf power by a klystronlike amplifier,” *Rev. Sci. Instrum.*, vol. 61, no. 1, pp. 171–181, Jan. 1990, doi: 10.1063/1.1141869.

[4] C. Chang *et al.*, “Design and experiment of the GW high power microwave feed horn,” *Prog. Electromagn. Res.*, vol. 101, pp. 157–171, Jan. 2010, doi: 10.2528/PIER10010202.

[5] C. Chang, G. Liu, C. Tang, C. Chen, and J. Fang, “Review of recent theories and experiments for improving high-power microwave window breakdown thresholds,” *Phys. Plasmas*, vol. 18, no. 5, May 2011, Art. no. 055702, doi: 10.1063/1.3560599.

[6] J. A. Swegle, E. Schamiloglu, and J. Benford, *High Power Microwaves*. New York, NY, USA: Taylor & Francis, 2007, pp. 1–8.

[7] C. Chang *et al.*, “A compact two-way high power microwave combiner,” *Rev. Sci. Instrum.*, vol. 85, no. 8, Aug. 2014, Art. no. 084704, doi: 10.1063/1.4891698.

[8] C. Chang *et al.*, “Compact four-way microwave power combiner for high power application,” *J. Appl. Phys.*, vol. 115, no. 21, Jun. 2014, Art. no. 055702, doi: 10.1063/1.4880741.

[9] X. Q. Li, Q. X. Liu, J. Q. Zhang, and L. Zhao, “16-element single-layer rectangular radial line helical array antenna for high-power application,” *IEEE Antennas Wireless Propag. Lett.*, vol. 9, pp. 708–711, 2010, doi: 10.1109/LAWP.2010.2059371.

[10] T. Mitha and M. Pour, “Investigation of dominant transverse electric mode in microstrip patch antennas,” *IEEE Trans. Antennas Propag.*, vol. 67, no. 1, pp. 643–648, Jan. 2019.

[11] Y. Xu *et al.*, “Design and test of broadband rectangular waveguide TE_{10} to circular waveguide TE_{21} and TE_{01} mode converters,” *IEEE Trans. Electron Devices*, vol. 66, no. 8, pp. 3573–3579, Aug. 2019.

[12] Q. Zhang, C.-W. Yuan, and L. Liu, “A dual-band coaxial waveguide mode converter for high-power microwave applications,” *Chin. Phys. Lett.*, vol. 28, no. 6, Jun. 2011, Art. no. 068401, doi: 10.1088/0256-307x/28/6/068401.

[13] V. L. Bratman *et al.*, “Generation of 3 GW microwave pulses in X-band from a combination of a relativistic backward-wave oscillator and a helical-waveguide compressor,” *Phys. Plasmas*, vol. 17, no. 11, Nov. 2010, Art. no. 110703, doi: 10.1063/1.3505825.

[14] B. Lee, W. Lee, Y. Yoon, and J. So, “X-band TM_{01}-TE_{11} mode converter with short length for high power,” *Electron. Lett.*, vol. 40, no. 18, pp. 1126–1127, 2004, doi: 10.1049/el:20045306.

[15] A. Chittora, J. Mukherjee, S. Singh, and A. Sharma, “Dielectric loaded TM_{01} to TE_{11} mode converter for S-band applications,” *IEEE Trans. Dielectr. Electr. Insul.*, vol. 22, no. 4, pp. 2057–2063, Aug. 2015, doi: 10.1109/TDEI.2015.005038.

[16] M. M. Honari, R. Mirzavand, S. Aslanzadeh, H. Saghlatoon, and P. Mousavi, “Wideband printed TM_{01} to TE_{11} mode converters,” *IEEE Access*, vol. 7, pp. 35438–35448, 2019, doi: 10.1109/ACCESS.2019.2904247.

[17] D. Wang, F. Qin, S. Xu, A. Yu, and Y. Wu, “Investigation of a metallic photonic crystal high power microwave mode converter,” *AIP Adv.*, vol. 5, no. 2, Feb. 2015, Art. no. 027102, doi: 10.1063/1.4907750.

[18] D. Goebel, R. Schumacher, and R. Eisenhart, “Performance and pulse shortening effects in a 200-kV PASOTRON^{TM} HPM source,” *IEEE Trans. Plasma Sci.*, vol. 26, no. 3, pp. 354–365, Jun. 1998, doi: 10.1109/27.700766.

[19] Z. Yang, C. Ge, and Z. Liang, “An unmagnetized plasma-loaded relativistic backward-wave oscillator: Experiment and simulation,” *Int. J. Infr. Millim. Waves*, vol. 21, no. 11, pp. 1887–1896, Jul. 2000, doi: 10.1023/a:1006748306402.

[20] D. Goebel, J. Butler, R. Schumacher, J. Santoru, and R. Eisenhart, “High-power microwave source based on an unmagnetized backward-wave oscillator,” *IEEE Trans. Plasma Sci.*, vol. 22, no. 5, pp. 547–553, 1994, doi: 10.1109/27.338267.

[21] S. H. Gold and G. S. Nusinovich, “Review of high-power microwave source research,” *Rev. Scientific Instruments*, vol. 68, no. 11, pp. 3945–3974, Nov. 1997, doi: 10.1063/1.1148382.

[22] S. A. Naqvi, G. S. Kerslick, J. A. Nation, and L. Schächter, “Axial extraction of high–power microwaves from relativistic traveling wave amplifiers,” *Appl. Phys. Lett.*, vol. 69, no. 11, pp. 1550–1552, Sep. 1996, doi: 10.1063/1.117058.

[23] R. J. Barker and E. Schamiloglu, “Windows and RF breakdown,” in *Proc. High-Power Microw. Sour. Technol.*, May 2001, pp. 325–375.